# A Temperature-Dependent Dielectric Model for Thawed and Frozen Organic Soil at 1.4 GHz

Valery L. Mironov, *Member, IEEE*, Yann H. Kerr, *Senior Member, IEEE*, Liudmila G. Kosolapova, Igor V. Savin, and Konstantin V. Muzalevskiy, *Member, IEEE*

***Abstract*—A single-frequency dielectric model for thawed and frozen Arctic organic-rich (80%–90% organic matter) soil was developed. The model is based on soil dielectric data that were measured over the ranges of volumetric moisture from 0.007 to 0.573 cm$^3$/cm$^3$, dry soil density from 0.564 to 0.666 g/cm$^3$, and temperature from 25 °C to –30 °C (cooling run), at the frequency of 1.4 GHz. The refractive mixing model was applied to fit the measurements of the soil's complex refractive index (CRI) as a function of soil moisture, with the values of temperature being fixed. Using the results of this fitting, the parameters of the refractive mixing model were derived as a function of temperature. These parameters involve the CRIs of soil solids as well as bound, transient, and free soil water components. The error of the dielectric model was evaluated by correlating the predicted complex relative permittivity (CRP) values of the soil samples with the measured ones. The coefficient of determination ($R^2$) and the root-mean-square error (RMSE) were estimated to be $R^2 = 0.999$, RMSE $= 0.27$ and $R^2 = 0.993$, RMSE $=$ 0.18 for the real and imaginary parts of the CRP, respectively. These values are in the order of the dielectric measurement error itself. The proposed dielectric model can be applied in active and passive remote-sensing techniques used in the areas with organic-rich soil covers, mainly for the SMOS, SMAP, and Aquarius missions.**

***Index Terms*—Dielectric constant, dielectric losses, dielectric measurement, L-band, modeling, soil moisture, soil properties.**

## I. Introduction

L-BAND radiometry is the most promising remote-sensing technique for monitoring the soil moisture over land surfaces. The dielectric models of moist soils are an essential part of this technique. The spectroscopic dielectric model for a set of mineral soils at the temperature of ~20 °C was developed in [1]. This model, with wave frequency, moisture, and clay percentage being the only input parameters, was shown to provide dielectric predictions with noticeably smaller error, compared to the dielectric predictions provided by the earlier suggested Dobson's model [2]. The latter is similar to the model of [1] in terms of the input parameters and the output products, despite being different in its concept. In the case of thawed mineral soils, the model of [1] was modified in [3] to introduce temperature as one more input parameter. In this form, the temperature and mineralogy-dependent spectroscopic dielectric model for the thawed mineral soils, as developed in [3], was implemented in the data-processing algorithm of the Soil Moisture and Ocean Salinity (SMOS) space mission. Currently, the SMOS soil moisture retrieval algorithm [4] is being extensively validated over a wide variety of land covers [5]–[7]. At the same time, new land covers as well as new land parameters, which were not initially considered as the SMOS mission targets, have recently started to emerge. Among those new land covers are boreal forest and arctic tundra territories [8], and one of the new parameters is the temperature profiles in the frozen active layer of permafrost [9]. To address these possible targets for the SMOS mission, the respective dielectric models for the thawed and frozen organic-rich soils must be available. Currently, the only dielectric model for an organic-rich Arctic soil, both thawed and frozen, was developed in [10].

The dielectric models developed in [1] and [10] are theoretically based on the well-known refractive mixing dielectric model (RMDM), which represents the complex refractive index (CRI) of moist soil as a sum of the CRIs related to the solid particles, water, and air constituents that are weighted by the respective volumetric contents of each constituent. The parameters of the RMDM are the CRIs of the soil constituents. The RMDM was initially proposed in [11]. Later, a spectral version of the RMDM was developed in [12]. The latter is currently known as the generalized refractive mixing dielectric model (GRMDM), which contains such spectral parameters as the low-frequency limit dielectric constant, dielectric relaxation time, and electrical conductivity related to different components of soil water. As a result, the dielectric model of [12] provides predictions for the soil complex relative permittivity (CRP) spectra in a certain frequency band for given values of soil moisture and temperature. The concepts of the dielectric models in [1] and [10] are the same as those of the GRMDM. Moreover, the dielectric model developed in [10] is a temperature-dependent spectral dielectric model. The temperature dependence of moist soil CRP in [10] is ensured due to use of the equation by Clausius–Mossotty for the low-frequency dielectric constant, the Debye equation for the dielectric relaxation time, and a linear dependence on temperature for the soil water ionic conductivity. As a result, the soil CRP temperature

Manuscript received January 29, 2015; revised May 04, 2015; accepted June 03, 2015. Date of publication August 23, 2015; date of current version December 21, 2015. This work was supported in part by a grant from the Russian Science Foundation under Project 14-17-00656. *(Corresponding author: Liudmila G. Kosolapova.)*

V. L. Mironov, L. G. Kosolapova, I. V. Savin, and K. V. Muzalevskiy are with Kirensky Institute of Physics, Krasnoyarsk 660036, Russia (e-mail: rsdvk@ksc.krasn.ru).

Y. H. Kerr is with the National Center for Scientific Research, Laboratory CESBIO UMR, 31404 Toulouse Cedex 9, France (e-mail: Yann.kerr@cesbio.cnes.fr).

Digital Object Identifier 10.1109/JSTARS.2015.2442295

dependences appeared to be available in the form of analytical expressions containing a set of thermodynamics parameters, which are derived using the measured dependences on the temperature for moist soil CRPs.

The dielectric model of [10] provides the CRP predictions for an organic-rich Arctic soil in the range of wave frequency from 1.0 to 16 GHz and in the temperature ranges from $-6\,^{\circ}\mathrm{C}$ to $25\,^{\circ}\mathrm{C}$ and from $-30\,^{\circ}\mathrm{C}$ to $-7\,^{\circ}\mathrm{C}$, corresponding to the cases of thawed and frozen soils, respectively. The dielectric measurements in [10] were conducted in a cooling run using a closed measurement container, in which a supercooled form of soil water existed in the temperature range of $0\,^{\circ}\mathrm{C}$ to $-6\,^{\circ}\mathrm{C}$. However, the organic topsoil in the tundra becomes frozen at the negative centigrade temperatures that are close to $0\ ^{\circ}\mathrm{C}$. As a result, in the dielectric model of [10], the temperature interval $-0\ ^{\circ}\mathrm{C}$ to $-6\ ^{\circ}\mathrm{C}$ in the case of frozen soil appeared to be missing. This feature of the dielectric model in [10] does not allow for prediction of the CRPs for a frozen soil in the temperature interval where the variations of soil CRP with temperature are most noticeable. To remove this restriction, the dielectric model of [10] should be modified before it is applied in the remote-sensing retrieval algorithms.

However, regarding retrieval algorithms using sensors data obtained at a single frequency, an alternative approach, relative to the spectral dielectric modes considered in [1] and [10], can be used to develop the respective single-frequency dielectric models. These models are much simpler than the spectral ones developed in [1] and [10]. A single-frequency dielectric model can be based on the RMDM, so that the CRIs of the soil constituents and their contents in the soil become the only parameters to be derived from dielectric measurements. The formulation of a single-frequency dielectric model, as well as the procedure of retrieving its parameters, is much simpler compared to the GRMDM of [1] and the temperature-dependent GRMDM of [10] because their spectroscopic and thermodynamic parameters are derived with much additional effort.

In this paper, a single-frequency dielectric model at 1.4 GHz for the soil earlier studied in [10] was developed. In the model, the temperature range of $-1\ ^{\circ}\mathrm{C}$ to $-6\ ^{\circ}\mathrm{C}$ is considered in the case of frozen soil samples. At the same time, the variations in soil dry density with temperature were neglected, as in [10]. The suggested dielectric model aims at applications in the case of organic-rich Arctic soils for developing algorithms to retrieve near-surface soil moisture or even derive temperature profiles in a frozen topsoil layer, using the brightness temperature and the backscatter coefficient data of the SMOS, SMAP, and other missions.

## II. Experimental Data and the RMDM

To develop the dielectric model, we used samples of Arctic soil that were collected on shrub tundra in Alaska [13] and earlier analyzed in [10]. The percentages of organic matter and mineral solids in the soil are the following: 80%–90%—organic matter, 4.5%—tiff, 7.5%–8.2%—quartz, 0.75%—plagioclase, 0.75%–1.5%—mica, and 0.75%—smectite. Before performing the dielectric measurements, the samples were ground using a coffee grinder. The crushed samples were dried in an oven at $104\ ^{\circ}\mathrm{C}$ for 24 h prior to the dielectric measurements. Next, a predetermined amount of distilled water is added to each specific soil sample. The resulting combination was mixed well and then stored in a sealed container for another 24 h. To conduct dielectric measurements, the soil sample was placed into a cell formed by a section of coaxial waveguide with the cross section of 7/3 mm, the latter ensuring that only the TEM mode is in the measured frequency range. The length of sample placed in the cell and its volume were equal to 17 mm and $0.529\,\mathrm{cm}^3$, respectively. When filling the measurement cell, the soil was compacted with a cylinder pestle. The cell was blocked on both sides with teflon washers, which prevented the sample from changing in volume. The cell was connected to the ZVK Rohde & Schwarz vector network analyzer to measure the frequency spectra of the S11, S22, S12, and S21 elements of the scattering matrix S over the frequency range from 50 MHz to 16 GHz. The isothermal measurements were ensured with the use of an SU-241 Espec chamber of heat and cold with accuracy $0.5\ ^{\circ}\mathrm{C}$. To control the isothermal measurements, a combined system consisting of the chamber and the network analyzer was developed, using the RS-232 interface and a set of built-in commands. This system allows for setting a sequence of temperatures at which the spectra of the scattering matrices are measured isothermally. After the temperature control system switches the chamber to a next assigned temperature point and this temperature is established inside the chamber, the system starts controlling the root-mean-square deviations between the S12 spectra subsequently measured every minute. When the value of the root-mean-square deviation decreases to below 0.01, the system switches the chamber to the next assigned temperature point, and the process of establishing temperature equilibrium between the sample and the chamber at the assigned temperature point repeats. An interval of time to transfer from one measurement temperature to another is maximal at the largest moisture of the soil sample, taking the following values: 1) 10 min in the case of thawed soil; 2) 40 and 20 min in the case of frozen soil for the temperature intervals of $-15\ ^{\circ}\mathrm{C} < \mathrm{T} < -1\ ^{\circ}\mathrm{C}$ and $-30\ ^{\circ}\mathrm{C} < \mathrm{T} < -15\ ^{\circ}\mathrm{C}$, respectively. The algorithm developed in [14] was applied to retrieve the spectra of the CRP of moist sample using the measured values of S11 and S12 or S22 and S21. This algorithm provides the real and imaginary parts of the CRP, with the errors less than 10%.

As in [10], we analyze the soil CRP $\varepsilon^*$, in terms of the reduced CRI

$$(n^* - 1)/\rho_d = (\sqrt{\varepsilon^*} - 1)/\rho_d = (n - 1)/\rho_d + i\kappa/\rho_d \quad (1)$$

where $n = \mathrm{Re}\sqrt{\varepsilon^*}$ and $\kappa = \mathrm{Im}\sqrt{\varepsilon^*}$ are the real and imaginary parts of CRI, respectively. $\rho_d$ is the density of the dry soil. In the framework of the RMDM as formulated in [10], the reduced CRI does not depend on the dry soil density. Furthermore, the gravimetric moisture of the soil samples $m_g$, which is the ratio of the mass of soil water to that of the dry soil sample,

TABLE I
DEPENDENCE OF THE DRY SOIL DENSITY $\rho_d$ AND VOLUMETRIC MOISTURE $m_v$ ON SOIL GRAVIMETRIC MOISTURE $m_g$

| | | | | | | | | |
|---|---|---|---|---|---|---|---|---|
| $m_g$(g/g) | 0.01 | 0.106 | 0.126 | 0.144 | 0.176 | 0.202 | 0.237 | 0.263 |
| $\rho_d$(g/cm$^3$) | 0.666 | 0.622 | 0.625 | 0.591 | 0.604 | 0.568 | 0.564 | 0.566 |
| $m_v$(cm$^3$/cm$^3$) | 0.007 | 0.066 | 0.079 | 0.085 | 0.106 | 0.115 | 0.134 | 0.149 |
| $m_g$(g/g) | 0.339 | 0.377 | 0.385 | 0.382 | 0.441 | 0.562 | 0.763 | 0.942 |
| $\rho_d$(g/cm$^3$) | 0.581 | 0.564 | 0.574 | 0.595 | 0.601 | 0.596 | 0.603 | 0.608 |
| $m_v$(cm$^3$/cm$^3$) | 0.197 | 0.213 | 0.221 | 0.227 | 0.265 | 0.335 | 0.46 | 0.573 |

can be the only variable when fitting the reduced CRI measured as a function of gravimetric moisture and dry soil density. Varying values of dry soil density in the measured samples arise when the soil substance, having different amounts of water, is packed into a measurement coaxial cell. Therefore, the soil density in the measured samples depends on its initial moisture, i.e., $\rho_d = \rho_d(m_g)$. This dependence was measured; the density of the dry soil samples as a function of gravimetric $m_g$ and volumetric $m_v = m_g\rho_d(m_g)$ moisture is presented in Table I.

A number of moisture dependencies of the reduced CRIs were measured for the thawed and frozen soil samples at the wave frequency $f$ of 1.4 GHz and at fixed temperatures $T$ in the ranges $0\ ^\circ\text{C} \le T \le 25\ ^\circ\text{C}$ and $-30\ ^\circ\text{C} \le T \le -7\ ^\circ\text{C}$. Some of those dependencies are shown in Fig. 1.

Fig. 1 shows, along with the measured data, the fits obtained with the use of the RMDM, as given in (2) and (3), shown at the bottom of the page.

The subscripts $s$, $d$, $m$, $b$, $t$, $l$, and $i$ (which are related to $n$, $\kappa$, and $\rho$) refer to the moist soil, dry soil, solid component of soil, bound water, transient water, free-liquid water, and ice, respectively. $m_{g1}$, and $m_{g2}$ are the maximum gravimetric fractions of the bound water and of the total bound water (consisting of bound water and transient water), respectively. The parameter $m_{g1}$ separates the range of bound water from that of transient water. In addition, $m_{g2}$ separates the region of transient water from that of free water that exists in a form of liquid water and ice in the case of thawed and frozen soil, respectively. The first, second, and third equations in formulas (2) and (3) must be applied in the ranges of bound water $m_g \le m_{g1}$, transient water $m_{g1} \le m_g \le m_{g2}$, and free-liquid water $m_g \ge m_{g2}$, respectively.

As observed from Fig. 1, the fits derived with the use of formulas (2) and (3) perfectly correspond to the measured data. These dependencies have the form of piecewise linear functions, with each specific segment of the polyline (jogged line) corresponding to a particular component of water. As a result of fitting, the parameters $(n_q - 1)/\rho_q$ and $\kappa_q/\rho_q$ concerning the solid component of the soil ($q = m$) and all the specific components of soil water ($q = b,\ t,\ l, i$), alongside with the maximum water fractions $m_{g1}$ and $m_{g2}$, were determined as a function of temperature.

In formulas (2) and (3), the dry soil density $\rho_d(m_g)$ was assumed to be independent of temperature. In this connection, note that a closed container manufactured of brass was used for the dielectric measurements. As follows from the respective estimates, the volume of the closed container and, consequently, the dry soil sample density altered by only 0.1% in the course of decreasing the temperature from $25\ ^\circ\text{C}$ to $-30\ ^\circ\text{C}$. Therefore, the variations in dry soil density in the course of freezing were neglected.

## III. TEMPERATURE-DEPENDENT DIELECTRIC MODEL

We obtained the temperature dependences for all of the parameters in formulas (2) and (3) based on the totality of the measured dielectric data, such as those shown in Fig. 1, and using the procedure of fitting. The parameters $m_{g1}$, $m_{g2}$, $(n_m - 1)/\rho_m$, $(n_b - 1)/\rho_b$, $(n_t - 1)/\rho_t$, $(n_{l,i} - 1)/\rho_{l,i}$, $\kappa_m/\rho_m$, $\kappa_b/\rho_b$, $\kappa_t/\rho_t$, and $\kappa_{l,i}/\rho_{l,i}$ were derived by jointly fitting the formulas (2) and (3) directly to the two sets of measured data, i.e., $(n_s - 1)/\rho_d$ and $\kappa_s/\rho_d$ as a function of gravimetric moisture at the temperatures $0\ ^\circ\text{C}, 5\ ^\circ\text{C}, 10\ ^\circ\text{C}, 15\ ^\circ\text{C}, 20\ ^\circ\text{C}$, and $25\ ^\circ\text{C}$, and $-30\ ^\circ\text{C}, -25\ ^\circ\text{C}, -20\ ^\circ\text{C}, -15\ ^\circ\text{C}, -10\ ^\circ\text{C}$, and $-7\ ^\circ\text{C}$ in the cases of thawed and frozen soil, respectively. The number of parameters in formulas (2) and (3) is equal to 10, while the number of data points to be fitted for the real and imaginary parts of the CRI at a predetermined temperature is equal to 34, as shown in Fig. 1. With the ratio 10/34 between the number of parameters to be derived from fitting and the number of data points to be fitted at every temperature, we obtained the datasets related to each parameter in formulas (2) and (3), and, in turn, consisting of six data points corresponding to the measured temperatures. Next, the datasets thus obtained were fitted as a function of temperature, separately in the cases of

$$\frac{n_s - 1}{\rho_d(m_g)} = \begin{cases} \frac{n_m-1}{\rho_m} + \frac{(n_b-1)}{\rho_b} m_g, & m_g \le m_{g1} \\ \frac{n_m-1}{\rho_m} + \frac{(n_b-1)}{\rho_b} m_{g1} + \frac{(n_t-1)}{\rho_t}(m_g - m_{g1}), & m_{g1} \le m_g \le m_{g2} \\ \frac{n_m-1}{\rho_m} + \frac{(n_b-1)}{\rho_b} m_{g1} + \frac{(n_t-1)}{\rho_t}(m_{g2} - m_{g1}) + \frac{n_{l,\,i}-1}{\rho_{l,\,i}}(m_g - m_{g2}), & m_g \ge m_{g2} \end{cases} \quad (2)$$

$$\frac{\kappa_s}{\rho_d(m_g)} = \begin{cases} \frac{\kappa_m}{\rho_m} + \frac{\kappa_b}{\rho_b} m_g, & m_g \le m_{g1} \\ \frac{\kappa_m}{\rho_m} + \frac{\kappa_b}{\rho_b} m_{g1} + \frac{\kappa_t}{\rho_t}(m_g - m_{g1}), & m_{g1} \le m_g \le m_{g2} \\ \frac{\kappa_m}{\rho_m} + \frac{\kappa_b}{\rho_b} m_{g1} + \frac{\kappa_t}{\rho_t}(m_{g2} - m_{g1}) + \frac{\kappa_{l,\,i}}{\rho_{l,\,i}}(m_g - m_{g2}), & m_g \ge m_{g2} \end{cases} \quad (3)$$

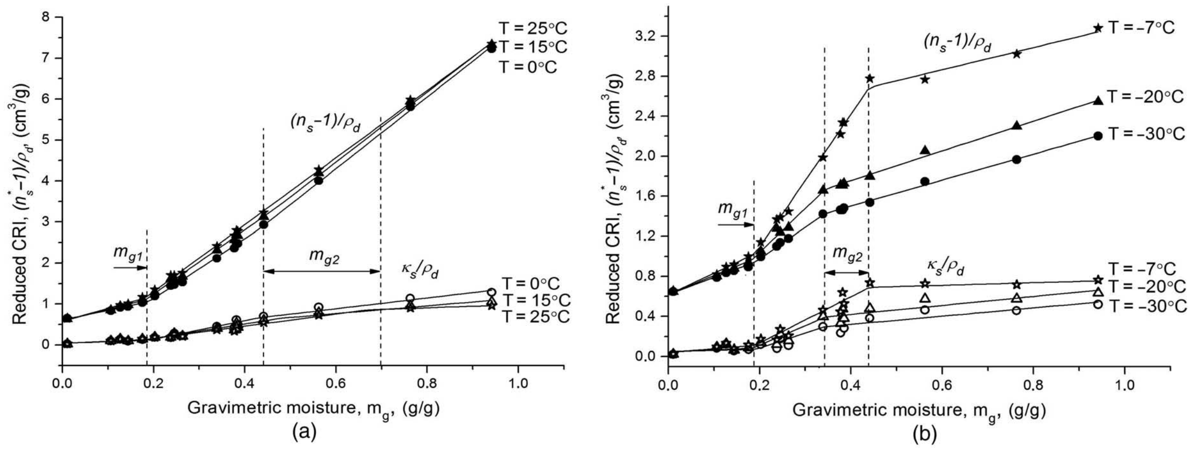


Fig. 1. Reduced CRI of soil as a function of gravimetric moisture at the frequency of 1.4 GHz. (a) Thawed soil. (b) Frozen soil. The measured temperatures are given by inscriptions. The values of $\rho_d(m_g)$ are given in Table I. The measured CRI values are shown by symbols. The piecewise linear fits are shown by solid lines.

thawed and frozen soil samples, using the functions described as follows:

$$\begin{aligned}
&\textbf{\textit{Thawed soil}}\\
&\mathbf{0\,^\circ C \le T \le +25\,^\circ C}\\
&m_{g1} = 0.185\\
&m_{g2} = 0.43 + 0.004\exp(T/6);\\
&(n_m - 1)/\rho_m = 0.62 - 0.002T;\\
&(n_b - 1)/\rho_b = 2.36 + 0.032T;\\
&(n_t - 1)/\rho_t = 7.37 + 0.032T;\\
&(n_l - 1)/\rho_l = 8.8 - 0.019T;\\
&\kappa_m/\rho_m = 0.04;\\
&\kappa_b/\rho_b = 0.463 + 0.0022T;\\
&\kappa_t/\rho_t = 2.23 - 0.03T;\\
&\kappa_l/\rho_l = 1.36 - 0.093\exp(T/11).
\end{aligned} \tag{4}$$

$$\begin{aligned}
&\textbf{\textit{Frozen soil}}\\
&\mathbf{-30\,^\circ C \le T \le -7\,^\circ C}\\
&m_{g1} = 0.185;\\
&m_{g2} = 0.335 + 0.095\exp(T/11);\\
&(n_m - 1)/\rho_m = 0.62;\\
&(n_b - 1)/\rho_b = 2.31 + 0.02T;\\
&(n_t - 1)/\rho_t = 7.71 + 0.16T;\\
&(n_i - 1)/\rho_i = 1.34 - 0.0026T;\\
&\kappa_m/\rho_m = 0.04 - 3.75\cdot 10^{-4}T;\\
&\kappa_b/\rho_b = 0.43 + 0.0115T;\\
&\kappa_t/\rho_t = 2.84 + 0.046T;\\
&\kappa_i/\rho_i = 0.45 - 0.15\exp(T/13).
\end{aligned} \tag{5}$$

Each function in (4) and (5) contains not more than three parameters that were derived based on six data points. Consequently, the number of recovered parameters in the temperature dependences of (4) and (5) is two or three times smaller compared to the number of fitted data points.

TABLE II
DENSITY OF DRY SOIL $\rho_d$ AND RESPECTIVE SOIL MOISTURES $m_g$ AND $m_v$ OBSERVED IN THE CASE OF VALIDATION MEASUREMENTS

| | | | | | | |
|---|---|---|---|---|---|---|
| $\boldsymbol{m_g}$(g/g) | 0.086 | 0.114 | 0.299 | 0.516 | 0.602 | 0.992 |
| $\boldsymbol{\rho_d}$(g/cm³) | 0.633 | 0.611 | 0.538 | 0.541 | 0.570 | 0.531 |
| $\boldsymbol{m_v}$(cm³/cm³) | 0.054 | 0.070 | 0.161 | 0.278 | 0.343 | 0.536 |

As observed from the formulas (4) and (5), the parameters of the developed model include separate formulas for the real $n$ and imaginary $\kappa$ parts of the CRI. These equations were derived based on the data for the real and imaginary parts of the CRIs of the soil samples that were jointly measured as independent values, using the phase shift and amplitude attenuation registered in a measuring coaxial line. Therefore, the real and imaginary parts of the reduced CRIs in (4) and (5) are considered as independent parameters of the developed dielectric model. However, providing that the influence of the quasi-static electrical conductivity of soil samples at a frequency of 1.4 GHz is strongly reduced, the real and imaginary parts of the soil CRP are linked to each other through the Kramers–Kronig relations [15]. The Kramers–Kronig relations imply that the real and imaginary parts of reduced CRIs in (4) and (5) must be interdependent. In principle, this interdependence could reduce the number of parameters of the developed dielectric model. However, in our approach, the reduction in the number of parameters was unnecessary because they all can be quite simply and directly determined from measurement data.

As follows from (5), the value of the CRI of ice is $n_i{}^* = 2.23 + 0.41i$ at the temperature $0\ ^\circ\mathrm{C}$. This CRI is greater than the one that is characteristic of crystal ice. The literature value for pure ice is $n^* = 1.78 + 0.0002i$, and even with saline inclusion, the imaginary part should be below 0.1 [16]. In this connection, we can assume that the ice in the soil pores is different from crystal ice. The ice particles in the soil pores may be

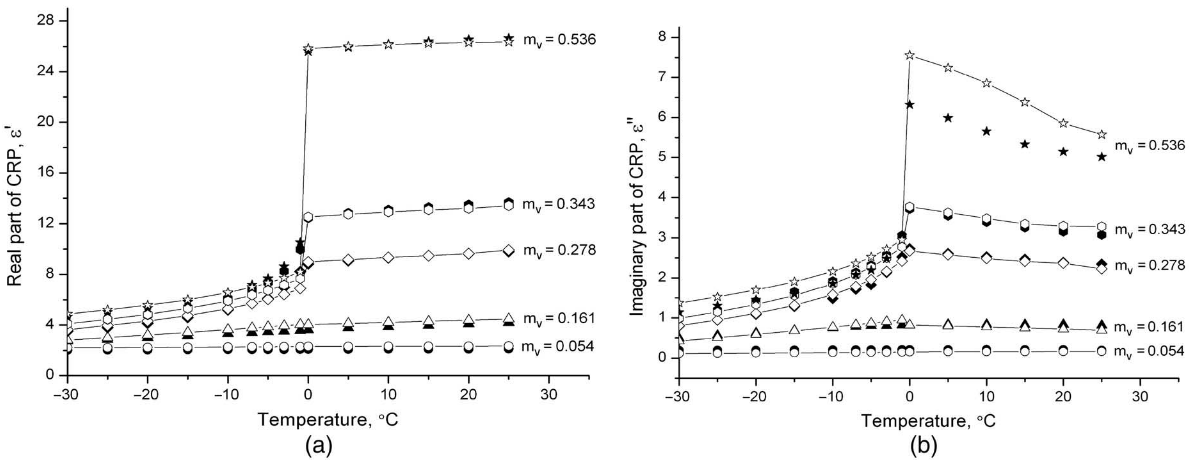


Fig. 2. CRP of moist soil as a function of temperature for fixed volumetric moistures $m_v$ (given by inscriptions) at the frequency of 1.4 GHz. The values of $\rho_d(m_v)$ are given in Table II. (a) Real part of the CRP $\varepsilon'$. (b) Imaginary part of the CRP $\varepsilon''$. The measured and predicted CRP values are shown by filled and open symbols, respectively. The solid lines correspond to the predicted CRPs.

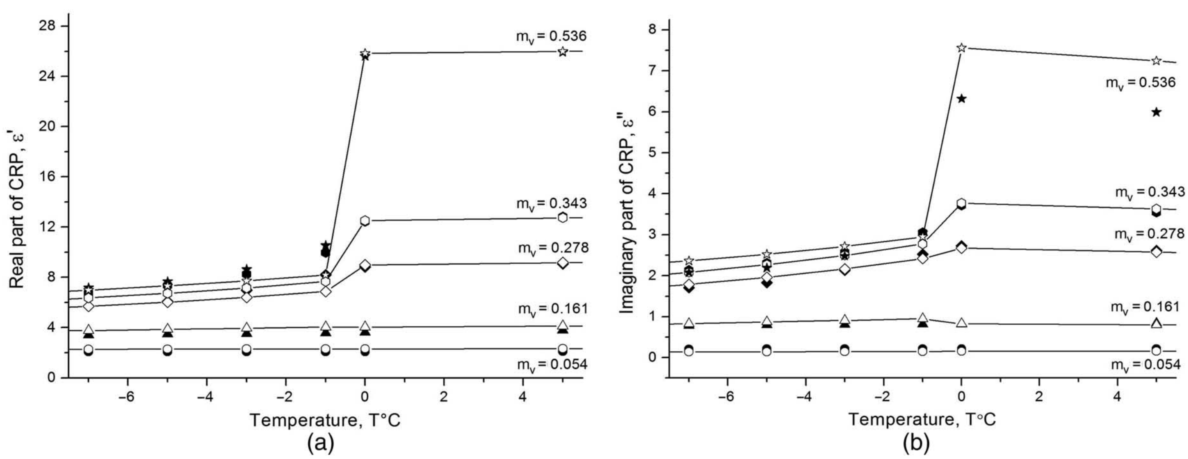


Fig. 3. Fig. 2 zoomed-in the temperature range over $-7\,°\mathrm{C}$ to $+5\,°\mathrm{C}$.

coated with unfrozen water films adsorbed onto the surface of the ice formations in the soil, similar to the bound water in soil adsorbed on the surface of the soil solids. Therefore, we cannot expect that the refractive index of ice in soil is equal to that of pure ice. Moreover, the unfrozen water on the surface of ice crystals is assumed to absorb the salt released from the liquid unbound soil water in the process of its turning into ice. As a result, a wet conglomerate of ice crystals formed from unbound salted water may have much larger imaginary part of the CRI than the pure ice. Of course, this hypothesis must be further investigated.

According to (1), the real $\varepsilon_s'$ and imaginary $\varepsilon_s''$ parts of the soil CRP can be expressed via the real $n_s$ and imaginary $\kappa_s$ parts of CRI as follows:

$$\varepsilon_s' = {n_s}^2 - {\kappa_s}^2, \quad \varepsilon_s'' = 2 n_s \kappa_s. \tag{6}$$

Equations (2)–(6) represent the temperature-dependent dielectric model for the CRP of both the thawed and frozen soil at the frequency of 1.4 GHz and in the ranges of temperature from $-30\,°\mathrm{C}$ to $-7\,°\mathrm{C}$ and $0\,°\mathrm{C}$ to $+25\,°\mathrm{C}$. To calculate the CRP as a function of gravimetric moisture using formulas in (2)–(6), one must assign the following variables: 1) dry soil density $\rho_d$; 2) gravimetric moisture $m_g$; and 3) temperature $T$.

Formulas (4) and (5) were obtained based on the measurements on the soil samples having the values of dry soil density that vary from 0.564 to 0.666 g/cm$^3$ (see Table I). However, taking into account that, according to formulas (2) and (3), the parameters of the RMDM are invariant with regard to the dry soil density, we assume that the formulas in (4) and (5) are applicable for other values of dry soil density that may be observed in nature. For the soil under study, the density of dry soil determined at the site of collection [10] equals $0.254\,\mathrm{g/cm^3}$. If the developed dielectric model is applied in remote-sensing retrieval algorithms, the data on the dry soil density should be taken from some data sources related to the surveyed territory.

In spite of the fact that the formulas (5) were obtained on the basis of dielectric data measured in the temperature range $-30\,°\mathrm{C} \le T \le -7\,°\mathrm{C}$, we assumed those to be applicable in the temperature range of $-7\,°\mathrm{C} < T \le -1\,°\mathrm{C}$ and validated the CRP values calculated under this assumption with the set

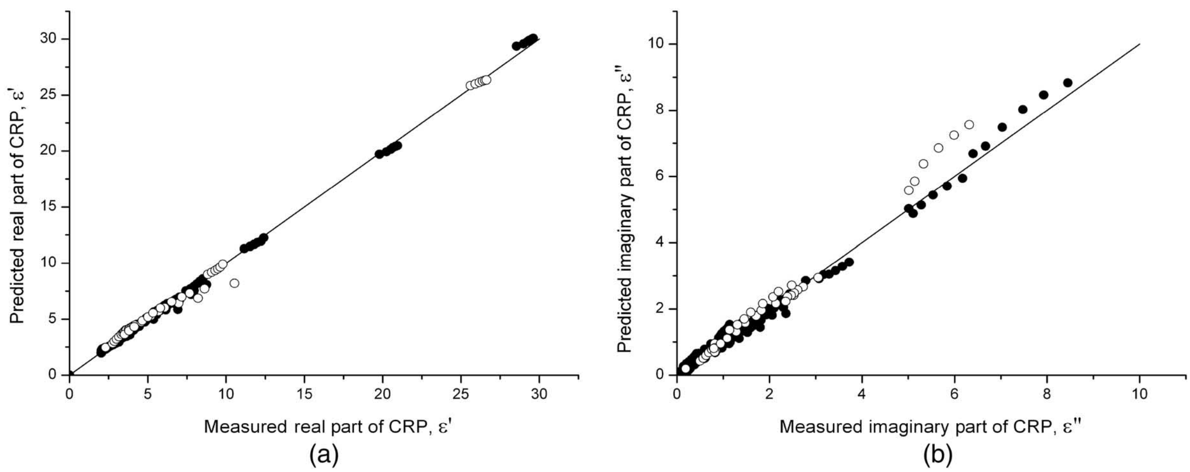


Fig. 4. Predicted CRPs of moist soil as a function of measured ones in the temperature ranges $-30\,^\circ\mathrm{C} \leq \mathrm{T} \leq -1\,^\circ\mathrm{C}$ and $0\,^\circ\mathrm{C} \leq \mathrm{T} \leq 25\,^\circ\mathrm{C}$. (a) Real part of CRP $\varepsilon'$.(b) Imaginary part of CRP $\varepsilon''$. The results corresponding to the additional measurements with $m_g$ and $\rho_d$ taken from Table II are shown by empty symbols. The bisectors are shown by solid lines.

of the CRPs especially measured in this range. This validation appeared to be successful, as outlined in Section IV.

## IV. Validation of the Dielectric Model

To conduct dielectric measurements for a frozen soil in the temperature range $-7\ ^\circ\mathrm{C} < T \leq -1\ ^\circ\mathrm{C}$, the process of ice nucleation was first induced using the temperature of $-7\ ^\circ\mathrm{C}$ and then completed using the temperature of $-1\,^\circ\mathrm{C}$. In the course of further cooling, measurements of soil CRPs at the temperatures of $-3\,^\circ\mathrm{C}$ and $-5\,^\circ\mathrm{C}$ were also conducted. All the remaining features of the measurement procedure were the same as discussed in Section II. For the additionally measured samples, the dry soil densities $\rho_d$ and respective soil moistures $m_g$ and $m_v$ are presented in Table II.

The results of the validation measurements for the soil CRP are shown in Figs. 2 and 3 as a function of temperature, together with the respective predictions obtained with the use of the formulas in (2)–(6).

As observed from Figs. 2 and 3, in the range of smaller moistures ($m_g \leq 0.161\,\mathrm{g/g}$), the predicted and measured CRP values are in good agreement. However, in the range of higher moistures ($m_g \geq 0.278\,\mathrm{g/g}$), the error increases as the temperature approaches the value of $-1\ ^\circ\mathrm{C}$.

To quantify the developed model error, we correlated the predicted CRPs with the total set of measured CRPs consisting of: 1) the CRPs that were used to derive (4) and (5); and 2) the additionally measured CRPs. In Fig. 4, the predicted values of the real part [Fig. 4(a)] and the imaginary part [Fig. 4(b)] of the CRP are shown versus the respective measured values. To estimate the error, we calculated the coefficient of determination for the real $\mathrm{R}^2_{\varepsilon'}$ and the imaginary $\mathrm{R}^2_{\varepsilon''}$ parts of the CRP, based on the data shown in Fig. 4; their values were found to be $\mathrm{R}^2_{\varepsilon'} = 0.999$ and $\mathrm{R}^2_{\varepsilon'} = 0.993$. The estimates of the RMSE of the predicted values relative to the measured ones for the real $\mathrm{RMSE}_{\varepsilon'}$ and imaginary $\mathrm{RMSE}_{\varepsilon''}$ parts of the CRP yielded the following values: $\mathrm{RMSE}_{\varepsilon'} = 0.27$ and $\mathrm{RMSE}_{\varepsilon''} = 0.18$, which are in the order of the dielectric measurement error itself.

## V. Conclusion

A temperature-dependent single-frequency dielectric model was developed for an organic-rich soil that was collected from a shrub tundra site located on the North Slope, Alaska. The model provides the CRPs of the thawed and frozen soil as a function of dry soil density, moisture, and temperature. The model was validated by the good agreement with the measured data for the wave frequency of 1.4 GHz, dry soil densities from 0.531 to 666 g/cm$^3$, volumetric moistures from 0.007 to 0.573 cm$^3$/cm$^3$, and temperatures from $-30\,^\circ\mathrm{C}$ to $+25\,^\circ\mathrm{C}$. With such wide variations of all of the input variables, the coefficients of determination for the real part of CRP $\mathrm{R}^2_{\varepsilon'}$ and the imaginary part of CRP $\mathrm{R}^2_{\varepsilon''}$ were found to be $\mathrm{R}^2_{\varepsilon'} = 0.999$ and $\mathrm{R}^2_{\varepsilon''} = 0.993$. The RMSEs of the predicted values of the real and imaginary parts of CRP relative to the measured values were found to be $\mathrm{RMSE}_{\varepsilon'} = 0.27$ and $\mathrm{RMSE}_{\varepsilon''} = 0.18$, respectively.

In terms of the error estimates, this model is appropriate because the values of its error are equal to the ones of the dielectric measurement itself. At the same time, regarding the applications of this model for developing the remote-sensing retrieval algorithms, the dielectric model is restricted to the investigated soil under the investigated laboratory conditions, which differ from the conditions observed in nature. The processing procedures used in the laboratory dielectric measurement, such as: 1) grinding soil solids; 2) drying organic soil at the temperature of $104\,^\circ\mathrm{C}$; and 3) compacting the soil solids in a coaxial measurement container, can modify the CRP of measured soil samples compared to the CRPs of natural plant materials. To ensure the applicability of the dielectric model for developing remote-sensing retrieval algorithms, the validation field experiments, which include measurements of brightness temperature and backscatter coefficient along with measurements of dry soil density, soil moisture, and soil temperature, are to be performed, and the deviations of the modeled values of brightness temperature and backscatter coefficient from the measured ones estimated. The above-described process is a routine procedure in developing adequate retrieval algorithms in soil moisture remote sensing with microwave radars and radiometers [17].

Furthermore, in real environmental conditions, the problem of the applicability of the developed dielectric model is more complicated because the soil cover in the Arctic tundra contains a wide variety of not only pure organic but also mixed composition soils. Therefore, a more general soil dielectric model that also accounts for soil solids composition is required, similar to the models in [3] and [18], which consider the thawed mineral soils. The latter models were successfully applied in the SMOS moisture retrieving algorithm [19]. In this view, the developed dielectric model is a reliable methodological basis for developing such a generalized dielectric model, which will eventually result in data-processing algorithms for modern remote-sensing missions, such as SMOS, SMAP, and Aquarius, relating to the organic-rich soil covers in Arctic areas. An advantage of the proposed dielectric model compared to the previous model of [10] is that a realistic soil freezing temperature of $-1\,^{\circ}\mathrm{C}$ was attained in a freezing run instead of a depressed soil freezing temperature of $-7\,^{\circ}\mathrm{C}$ that was inherent to the model of [10].

## REFERENCES


[1] V. L. Mironov, L. G. Kosolapova, and S. V. Fomin, "Physically and mineralogically based spectroscopic dielectric model for moist soils," *IEEE Trans. Geosci. Remote Sens.*, vol. 47, no. 7, pp. 2059–2070, Jul. 2009.

[2] M. C. Dobson, F. T. Ulaby, M. T. Hallikainen, and M. A. El-Rayes, "Microwave dielectric behavior of wet soil – Part II: Dielectric mixing models," *IEEE Trans. Geosci. Remote Sens.*, vol. GE-23, no. 1, pp. 35–46, Jan. 1985.

[3] V. L. Mironov and S. V. Fomin, "Temperature dependable microwave dielectric model for moist soils," in *PIERS Online*, vol. 5, no. 5, pp. 411–415, 2009.

[4] Y. H. Kerr *et al.*, "The SMOS soil moisture retrieval algorithm," *IEEE Trans. Geosci. Remote Sens.*, vol. 50, no. 5, pp. 1384–1400, May 2012.

[5] T. J. Jackson *et al.*, "Validation of soil moisture and ocean salinity (SMOS) soil moisture over watershed networks in the U.S," *IEEE Trans. Geosci. Remote Sens.*, vol. 50, no. 5, pp. 1530–1543, May 2012.

[6] A. Al Bitar *et al.*, "Evaluation of SMOS soil moisture products over continental U.S. using the SCAN/SNOTEL network," *IEEE Trans. Geosci. Remote Sens.*, vol. 50, no. 5, pp. 1572–1586, May 2012.

[7] S. Bircher, J. E. Balling, N. Skou, and Y. H. Kerr, "Validation of SMOS brightness temperatures during the HOBE airborne campaign, Western Denmark," *IEEE Trans. Geosci. Remote Sens.*, vol. 50, no. 5, pp. 1468–1482, May 2012.

[8] R. Rahmoune *et al.*, "SMOS retrieval results over forests: Comparisons with independent measurements," *IEEE J. Sel. Topics Appl. Earth Observ. Remote Sens.*, vol. 7, no. 9, pp. 3858–3866, Sep. 2014.

[9] V. L. Mironov, K. V. Muzalevskiy, and I. V. Savin, "Retrieving temperature gradient in frozen active layer of arctic tundra soils from radiothermal observations in L-band—Theoretical modeling," *IEEE J. Sel. Topics Appl. Earth Observ. Remote Sens.*, vol. 6, no. 3, pp. 1781–1785, Jun. 2013.

[10] V. L. Mironov, R. D. De Roo, and I. V. Savin, "Temperature-dependable microwave dielectric model for an arctic soil," *IEEE Trans. Geosci. Remote Sens.*, vol. 48, no. 6, pp. 2544–2556, Jun. 2010.

[11] J. R. Birchak, C. G. Gardner, J. E. Hipp, and J. M. Victor, "High dielectric constant microwave probes for sensing soil moisture," *Proc. IEEE*, vol. 62, no. 1, pp. 92–98, Jan. 1974.

[12] V. L. Mironov, M. C. Dobson, V. H. Kaupp, S. A. Komarov, and V. N. Kleshchenko, "Generalized refractive mixing dielectric model for moist soils," *IEEE Trans. Geosci. Remote Sens.*, vol. 42, no. 4, pp. 773–785, Apr. 2004.

[13] R. D. De Roo, A. W. England, H. Gu, H. Pham, and H. Elsaadi, "Ground based radiobrightness observations of the active layer growth on the north slope near Toolik Lake, Alaska," in *Proc. IEEE Int. Geosci. Remote Sens. Symp. (IGARSS)*, Denver, CO, USA, Jul. 31/Aug. 4, 2006, pp. 2708–2711.

[14] V. L. Mironov, S. A. Komarov, Y. I. Lukin, and D. S. Shatov, "A technique for measuring the frequency spectrum of the complex permittivity of soil," *J. Commun. Technol. Electron.*, vol. 55, no. 12, pp. 1368–1373, 2010.

[15] J. D. Jackson, *Classical Electrodynamics*. Hoboken, NJ, USA: Wiley, 1999, pp. 332–333. ISBN 0-471-43132-X.

[16] C. Mätzler *et al.*, *Thermal Microwave Radiation: Applications for Remote Sensing*. London, U.K.: Institution of Electrical Engineers, 2006.

[17] J.-P. Wigneron *et al.*, "Evaluating an improved parameterization of the soil emission in L-MEB," *IEEE Trans. Geosci. Remote Sens.*, vol. 49, no. 4, pp. 1177–1187, Apr. 2011.

[18] V. Mironov, Y. Kerr, J.-P. Wigneron, L. Kosolapova, and F. Demontoux, "Temperature and texture dependent dielectric model for moist soils at 1.4 GHz," *IEEE Geosci. Remote Sens. Lett.*, vol. 10, no. 3, pp. 419–423, May 2013.

[19] A. Mialon *et al.*, "Comparison of Dobson and Mironov dielectric models in the SMOS soil moisture retrieval algorithm," *IEEE Trans. Geosci. Remote Sens.*, vol. 53, no. 6, pp. 3084–3094, Jan. 2015.


**Valery L. Mironov** (M'98) received the M.S. and Ph.D degrees in radio physics from the Tomsk State University, Tomsk, Russia, in1961 and 1968, respectively.

He received the Full Professor degree in radio physics and was endorsed as a Correspondent Member Radio Physics by Russian Academy of Sciences, Moscow, Russia, in 1984 and 1991, respectively. Since 2004, he has been a Laboratory Head with Kirensky Institute of Physics, Siberian Branch of the Russian Academy of Sciences (SB RAS), Krasnoyarsk, Russia. From 1961 to 2004, he worked as a Researcher, Laboratory Head, Full Professor, and Chair Head with Tomsk State University, Altai State University, Barnaul, Russia, and the Institute of Atmospheric Optics, SB RAS. As a Visiting Scientist, he worked at the University of British Columbia, Vancouver, BC, Canada, and the Geophysical Institute, University of Alaska, Fairbanks, AK, USA, in 1997/1998 and 2001, respectively. In the period of last 10 years, he has authored more then 50 papers in the IEEE Journals and Conference Publications. In 2012, his temperature and mineralogy-dependent dielectric model of moist soils has been implemented as a part of the SMOS data-processing algorithm to retrieve soil moisture from the earth surface radiobrightness observations. His research interests include electromagnetic wave propagation and scattering linked to the radar and radio thermal microwave remote sensing of the land, including the studies of dielectric properties of moist soils.

Dr. Mironov is a Reviewer of the IEEE TRANSACTIONS ON GEOSCIENCE AND REMOTE SENSING, the IEEE GEOSCIENCE AND REMOTES SENSING LETTERS, the *International Journal of Remote Sensing*, and the *Remote Sensing of Environment*.

**Yann H. Kerr** (M'88–SM'01) received the Engineering degree in radar and telecommunications from Ecole Nationale Supérieure de l'Aéronautique et de l'Espace, Toulouse, France, the M.Sc. degree in electronics and electrical engineering from Glasgow University, Glasgow, U.K., and the Ph.D. degree in astrophysics, geophysics and space techniques from the Université Paul Sabatier, Toulouse, France.

From 1980 to 1985, he was employed by the Centre National d'Etudes Spatiales (CNES), Toulouse, France. In 1985, he joined the Laboratoire d'Etudes et de Recherche en Télédétection Spatiale, Toulouse, France; for which he was the Director in 1993–1994. He spent 19 months at Jet Propulsion Laboratories, Pasadena, CA, USA, in 1987–1988. He was an Earth Observing System Principal Investigator (interdisciplinary investigations) and Principal Investigator and precursor of the use of the Earth Resources Satellite SCAT terometer over land. In 1989, he started to work on the interferometric concept applied to passive microwave Earth observation and was subsequently the Science Lead on the Microwave Imaging Radiometer using Aperture Synthesis (MIRAS) project for European Space Agency (ESA) with Matra Marconi Space and Observatoire Midi Pyrénées. He was also a Co-Investigator on Inflatable Radiometric Imaging System, Optical System for Imaging and low-Intermediate-Resolution Integrated Spectroscopy, and Hydrosphere State for the National Aeronautics and Space Administration. He was a Science Advisor for Multifrequency Imaging Microwave Radiometer and Co-Investigator on Advanced Microwave Scanning Radiometer. He has been working with the Centre d'Etudes Spatiales de la BIOsphère since 1995 (Deputy Director and Director since 2007). In 1997, he first proposed the natural outcome of the previous MIRAS work with what was to become the Soil Moisture and Ocean Salinity (SMOS) Mission to CNES, proposal which was selected by ESA in 1999 with him as the SMOS mission Lead Investigator and Chair of the Science Advisory Group. He is also in charge of the SMOS science activities coordination in France. His research interests include the theory and techniques for microwave and thermal infrared remote sensing of the Earth, with emphasis on hydrology, water resources management, vegetation monitoring, exploitation of SMOS data, Cal Val activities, related level 2 soil moisture and level 3 and 4 development, SMOS next concept, and many space missions.

Dr. Kerr is a member of the Soil Moisture Active and Passive Science Definition Team. He has organized all the SMOS workshops and was a Guest Editor of three IEEE special issues.


**Liudmila G. Kosolapova** received the M.S. degree in mathematics from Krasnoyarsk State University, Krasnoyarsk, Russia, in 1971, and the Ph.D. degree in biophysics from the Institute of Biophysics of the Siberian Branch, Russian Academy of Sciences, Krasnoyarsk, Russia, in 1979.

Currently, she is a Senior Researcher with the Laboratory of Radiophysics of Remote Sensing, Kirensky Institute of Physics, Siberian Branch of the Russian Academy of Sciences (SB RAS), Krasnoyarsk, Russia. She is author/coauthor of over 70 scientific publications. Her research interests include simulation of the microwave dielectric properties of the soils, data processing, and dielectric models testing.

**Igor V. Savin** was born in Kurgan, Russia, in 1980. He received the Engineering degree in radio science from the Krasnoyarsk State Technical University, Krasnoyarsk, Russia, in 2002.

Currently, he is a Junior Researcher with Kirensky Institute of Physics, Siberian Branch of the Russian Academy of Sciences (SB RAS), Krasnoyarsk, Russia. He is also engaged in the development of dielectric measurement technique and instrumentation. He is the coauthor of 20 scientific publications. His research interests include dielectric properties of moist soils and rocks with alternating mineral contents and temperatures.

**Konstantin V. Muzalevskiy** (M'12) received the M.S. degree in radio science and electronics from the Altai State University, Barnaul, Russia, in 2004, and the Ph.D. degree in radiophysics from Kirensky Institute of Physics, Siberian Branch of the Russian Academy of Sciences (SB RAS), Krasnoyarsk, Russia, in 2010.

Since 2008, he is an Assistant Professor with Rehsetnev Siberian State Aerospace University, Krasnoyarsk, Russia. Since 2010, he is a Research Fellow with the Laboratory of Radiophysics of Remote Sensing, Kirensky Institute of Physics, SB RAS. He is the author/coauthor of over 50 scientific publications and a book *Ultrawideband Electromagnetic Sounding of a Oil-Saturated Reservoir* (Novosibirsk, Russia: Publishing House of the SB RAS, 2011) (in Russian).

Dr. Muzalevskiy was granted the Krasnoyarsk Science Foundation (2010, 2011), Prohorov's Foundation (2010), Foundation for Assistance to Small Innovative Enterprises in Science and Technology Grant (2009), and Russian Foundation for Basic Research (2009, 2012) as a Young Scientist and JAXA ALOS PI, RA'4 (2013). He is a Leader of the youth project of the "Creating the radar remote sensing technology for monitoring of a thermal behavior of a top layer of the Arctic tundra soil of the Siberia in the process of freezing and thawing."